Nonlinear microrheology of wormlike micelle solutions using ferromagnetic nanowire probes

Nathan Cappallo, Clayton Lapointe, Daniel H. Reich, and Robert L. Leheny
Department of Physics and Astronomy, Johns Hopkins University, Baltimore, Maryland 21218, USA
(Received 10 April 2007; revised manuscript received 3 August 2007; published 27 September 2007)

Ferromagnetic nanowires were employed to investigate the microrheology of wormlike micelle solutions composed of equimolar cetylpyridinium chloride–sodium salicylate. For a wire rotated about a short axis, the drag at low rotation rate ω_R is independent of ω_R and strongly temperature dependent, consistent with the macroscopic shear viscosity. Above a critical rotation rate ω_c, the drag is independent of temperature and decreases as a power law with increasing rate. The onset of nonlinear drag is characterized by a peak associated with contributions from extensional flow. Above ω_c, the fluid generates an additional torque that tilts the wire out of regions of high shear flow and that is interpreted as a consequence of a shear-induced transition to nematic order among the micelles. Rotation of the wire in response to this torque reveals directly the anisotropy of the drag in the nonlinear state.

DOI: 10.1103/PhysRevE.76.031505 PACS number(s): 83.80.Qr, 47.50.−d, 83.60.Df, 83.85.Cg

I. INTRODUCTION

Complex fluids, such as polymer and surfactant solutions, are often distinguished by unusual and dramatic flow properties [1]. In particular, they can show pronounced non-Newtonian behavior, which is characterized by a strain-rate-dependent effective viscosity. Often, the onset of the non-Newtonian response is coincident with flow-induced anisotropy in the fluid. In recent years, microrheology techniques have emerged as a powerful alternative to traditional methods for studying the rheology of complex fluids. In microrheology, micrometer-scale particles suspended in a fluid are used to investigate the local mechanical environment. Among the advantages of this approach over conventional rheometry are the ability to study small samples, to access higher-frequency mechanical response [2,3], and to vary the probe size relative to the intrinsic length scales of the fluid microstructure [4]. While the vast majority of microrheology has addressed the linear response of complex fluids, a number of recent studies have explored its potential for nonlinear rheology [5–7]. In this paper, we report experiments employing ferromagnetic nanowires to study the nonlinear microrheology of strongly non-Newtonian wormlike micelle solutions. Under strong flow, the solutions become anisotropic, and the flexibility afforded by manipulating the wires with external magnetic fields enables us to probe directly the solutions' viscous and elastic behavior along different directions relative to the flow. In doing so, we demonstrate a further advantage of microrheology for revealing the anisotropic properties of the nonlinear states of complex fluids under flow that would be difficult or impossible to access using conventional means.

Wormlike micelle solutions are aqueous solutions of surfactant molecules that self-assemble into long, flexible cylinders. At sufficiently high concentrations the cylinders entangle in a manner similar to long polymers. Unlike polymers, however, wormlike micelles break and reform, which leads to their characteristic linear and nonlinear rheology [8]. The linear shear response can be remarkably simple, with solutions behaving as Maxwell fluids [8]. The nonlinear rheology, however, can be complicated [9], and, depending on specifics of the solution, dramatic shear thinning [9–11], shear thickening [12], or even chaotic behavior [13] is observed. The shear thinning is often accompanied by shear banding [14–17], which some authors have identified with a transition to nematic order among the micelles [11,16,18]. Consequently, wormlike micelle solutions have become important model systems for nonlinear rheology and for shear-induced phase transitions [19–21]. In our microrheology experiments, the magnetic nanowires, which are suspended in a wormlike micelle solution that displays strong shear thinning, serve a dual purpose. First, when rotated at sufficient rates, they create a flow-induced state locally. Then, as microrheological probes, they interrogate the viscoelastic properties of this state. The fluid forces that the wires experience, including a torque that appears discontinuously at high rotation rates and tilts the wires out of regions of high shear, reveal unexpected features of the nonlinear state that we speculate result from nematic order of the micelles.

II. EXPERIMENTAL PROCEDURES

The fluids under study were equimolar aqueous solutions of surfactant, cetylpyridinium chloride (CPCl), and salt, sodium salicylate (NaSal), at a concentration c= 8.5 mM. The CPCl (98%) and NaSal (99%) were obtained from Alpha Aesar and used without further purification. Appropriate quantities of each were added to deionized water and mixed thoroughly to form the wormlike micelle solutions. Macroscopic rheometry shows that such solutions become shear thinning at high shear rate (i.e., display decreasing effective viscosity with increasing shear rate) [22,23]. To perform the microrheology experiments, we suspended in the solutions a dilute concentration of Ni nanowires with radius $R=175\pm25$ nm and lengths ranging from $L=5$ to 50 μm. The methods for fabricating the wires via electrochemical deposition into nanoporous templates, extracting the wires from the templates, and magnetizing the wires along their long axes have been described previously [24]. When the nanowires are magnetized, their large magnetic dipole moments ($\mu=3\times10^{-10}$ emu for a 10 μm wire [24]) enable us to apply

strong, quantitatively precise torques to suspended wires through external magnetic fields, and to extract viscoelastic properties of fluids from the rotational motion of the wires in response to these torques [25–27]. We note that this approach to microrheology is distinct from most previous studies, which have typically centered on the translational motion of nominally spherical particles, and such application of rotating anisotropic colloids to microrheology has only recently begun to be explored [28–30].

The non-Newtonian behavior of the wormlike micelle solutions was investigated by monitoring the nanowire rotation using high-speed video microscopy. The wires under study were far from any boundaries of the fluid (at least 300 μm) and from other suspended wires whose interactions might have affected their motion. The microscope was equipped with eight computer-controlled solenoids with soft iron cores positioned about the temperature-controlled sample stage to create arbitrarily oriented and spatially uniform fields with magnitudes up to 100 G and frequencies up to 500 Hz. Complementary measurements of the macroscopic shear viscosity of the solutions were performed using a stress controlled rheometer (Anton-Paar MCR 300) in a cone-and-plate geometry.

III. RESULTS AND DISCUSSION

A. Linear and nonlinear drag

We first discuss measurements in which a wire was subjected to magnetic fields of constant magnitude B, rotating at constant angular velocity ω_R. In steady state, the low-Reynolds-number environment dictated that the wire rotated in response to the field with its magnetic moment vector, and hence its long axis, lagging the field by an angle θ such that the magnetic torque and drag torque from the fluid balanced; i.e.,

$$\mu B \sin\theta = D\eta_d\omega_R, \tag{1}$$

where $D=\pi L^3/3[\ln(L/2R)-0.662]$ is the geometric drag coefficient for a cylinder rotating about a short axis [31], and η_d is the effective drag viscosity that in general depended on ω_R. As a diagnostic calibration of the technique, wires suspended in the viscous Newtonian liquid glycerol were similarly rotated at a constant rate. The measured viscosity, which was independent of rate up to the largest rotation rates, matched the macroscopic value of the glycerol's viscosity to within the systematic uncertainty in η_d of ± 20%, due primarily to the variability in the wire radius and its relationship to the magnetic dipole moment μ.

Figure 1(a) displays values of η_d for the wormlike micelle solution, determined using a wire with $L=16.7$ μm in a field $B=60$ G, as a function of ω_R at several temperatures. The wire was rotated at each frequency for sufficient time to allow any transient effects to decay and to assure that a steady-state angle θ was established. Further, a pause of several minutes was included before each change in frequency to allow the fluid to return to a quiescent state. At low ω_R, η_d adopts a rate-independent value that we associate with the zero-shear-rate viscosity of the fluid, η_0. This viscosity increases strongly with decreasing temperature, presumably as a consequence of the increase in average micelle length with decreasing temperature [8]. Figure 1(b) shows the macroscopic shear viscosity η measured rheometrically as a function of shear rate $\dot{\gamma}$, which similarly reveals a strongly temperature-dependent zero-shear-rate viscosity. However, the values of η_0 obtained from the nanowire rotation are consistently smaller than those measured macroscopically by roughly a factor of two. This discrepancy likely results from a depletion of micelles in the vicinity of the wire, a common effect in microrheology on polymeric solutions [32]. In the range around $c=8.5$ mM, η_0 of equimolar CPCl-NaSal solutions varies strongly with concentration, $\eta_0 \sim c^{5.8}$ [22], indicating that a modest depletion in local micelle concentration would account for the discrepancy.

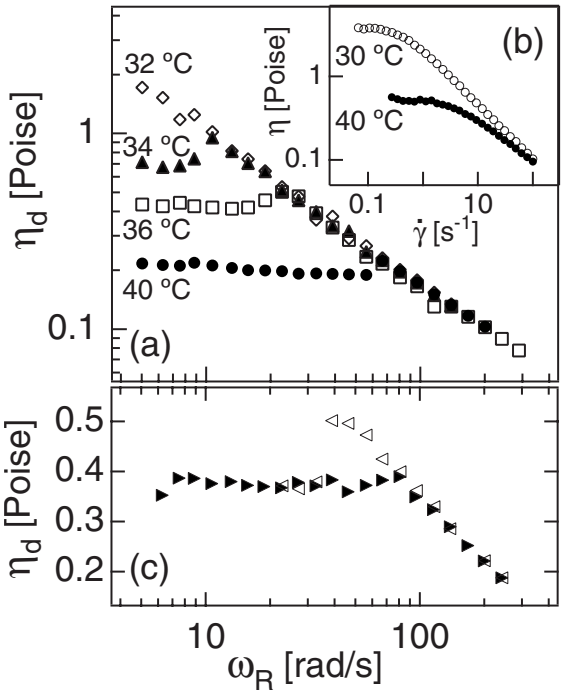

FIG. 1. (a) Drag viscosity of 8.5 mM CPCl-NaSal wormlike micelle solution determined from the rotation of a nanowire of length 16.7 μm as a function of rotation frequency at 32 (diamonds), 34 (triangles), 36 (boxes), and 40 °C (circles). (b) Viscosity of the solution determined using a stress-controlled rheometer with a cone-and-plate geometry as a function of shear rate at 30 (open) and 40 °C (filled). (c) Drag on a rotating nanowire of length 9.2 μm at 37 °C measured with no waiting time between frequencies on increasing (solid) and decreasing (open) rotation frequency.

At larger ω_R, η_d becomes nonlinear and decreases approximately as a power law, $\eta_d \sim \omega_R^{-0.75}$, above a sharply identified critical rotation rate ω_c that increases with increasing temperature. For a particle translating in a viscoelastic fluid, nonlinear behavior is typically measured in terms of the Deborah number, $\mathrm{De}=v\tau/a$, where v is the velocity, a is the particle size, and τ is a characteristic relaxation time. Nonlinear flow is generally expected for $\mathrm{De} > O(1)$. For our wormlike micelle solutions, measurements of stress relaxation indicate that $\tau \sim 1-10$ s at the temperatures in Fig. 1(a). Since the tip of a rotating wire moves at $v=\omega_R L/2$,

taking $a=R$, the wire radius, yields $\mathrm{De}\sim 10^3$ at ω_c, making the presence of the apparent linear regime in Fig. 1(a) surprising. However, unlike a translating particle, the segments of the rotating wire revisit the same region of fluid with a period π/ω_R, suggesting that $\omega_R\tau/\pi$ is a relevant quantity for characterizing the nonlinear behavior. Indeed, Fig. 1(a) indicates that nonlinear drag commences at $\omega_c\tau/\pi\sim O(1)$.

While this decreasing η_d at large ω_R appears similar to the shear thinning observed macroscopically at large $\dot{\gamma}$, where at 30 °C η at the highest shear rates decreases approximately as $\eta\sim\dot{\gamma}^{-0.7}$, a number of differences in the nonlinear regime also emerge [33]. First, the crossover to quasi-power-law dependence is less sharp in the rheometry than in the nanowire measurements. Also, above ω_c, η_d at different temperatures collapse onto a single curve, implying that $\eta_0\sim\omega_c^{-0.75}$ and in contrast to η, which remains temperature dependent in the nonlinear regime. Further, a small but distinct peak in η_d appears at the onset of the nonlinear regime, and no corresponding peak is observed in η. This peak in η_d becomes larger and extends to lower ω_R when measurements are obtained upon decreasing ω_R with no waiting time between frequencies. Figure 1(c) illustrates this hysteretic behavior.

These differences between the microrheology and shear rheometry are not entirely surprising. While their equivalence in linear response can be demonstrated rigorously, at least under ideal circumstances [34], such correspondence in the nonlinear response cannot in general be expected [6]. In fact, studies have shown how the nonlinear flow of a viscoelastic fluid past a cylinder can include strong extensional flow in the cylinder's wake [35]. The extensional viscosity of CPCl-NaSal solutions displays a sharp peak coincident with the onset of shear thinning [36]. (See Fig. 2 of Ref. [36].) Thus, we associate the peak in η_d with contributions from the extensional viscosity to the drag that enter in the nonlinear regime. While this identification illustrates the breakdown of the correspondence with macroscopic shear rheometry, it also highlights the unique perspective afforded by microrheology. Indeed, since the shear-thinning behavior in wormlike micelle solutions is associated with shear banding [14–17], one cannot expect a uniform shear rate in the nonlinear regime even for a cone-and-plate geometry, and η measured at high rates represents some combination of linear and nonlinear responses. The collapse of η_d at different temperatures in Fig. 1(a) thus illustrates a temperature invariance of the nonlinear state of the wormlike micelle solutions that is obscured in the macroscopic shear rheology.

B. Out-of-plane torque

Above ω_c, wires experience an additional force that highlights the anisotropic nature of the fluid's nonlinear state. Specifically, the fluid imparts a torque $\Gamma_\perp$ perpendicular to the drag torque that seeks to tilt the wires out of the rotation plane. Figures 2(a) and 2(b) display a pair of images that illustrates the effect of $\Gamma_\perp$. Figure 2(a) shows a wire as it rotates in the focal plane of the microscope in response to a rotating magnetic field at a frequency above ω_c. Figure 2(b) shows that, after removal of the field, the wire becomes oriented with its long axis perpendicular to the rotation plane as a consequence of $\Gamma_\perp$. The onset of this out-of-plane torque is very sharp as a function of ω_R and coincides with ω_c. In contrast, when a wire is rotated at $\omega_R<\omega_c$, the sense of rotation reverses immediately after removal of the field due to viscoelastic recoil, but the wire experiences no out-of-plane torque and remains in the rotation plane. Thus, we associate $\Gamma_\perp$ with the nonlinear state of the fluid. Figure 3 displays a "phase diagram" for this nonlinear behavior con-

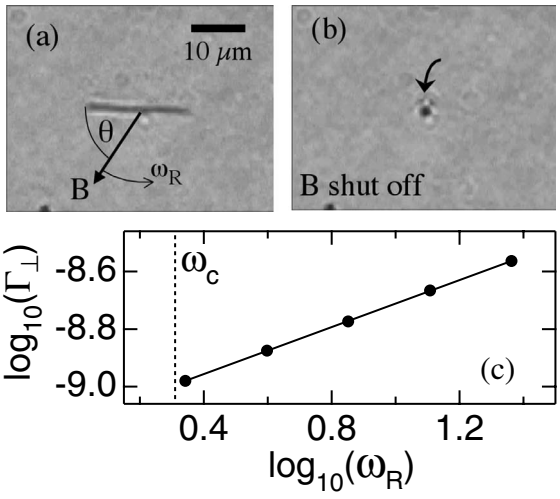

FIG. 2. (a) Micrograph of a rotating nanowire of length 19.0 μm following a field B rotating at frequency ω_R. (b) The same wire 0.2 s after removal of the field. The wire has tilted to an orientation perpendicular to the rotation plane in response to a torque from the fluid. (c) Values of the out-of-plane torque (in dyne cm) determined for a wire length 13.7 μm at 30 °C rotating at a constant out-of-plane tilt angle ($\phi=45°$) as a function of rotation frequency. The torque vanishes below a critical rotation frequency $\omega_c\approx 2.04$ rad/s. The solid line is the result of a power-law fit yielding $\Gamma_\perp\sim\omega_R^{0.40\pm0.05}$.

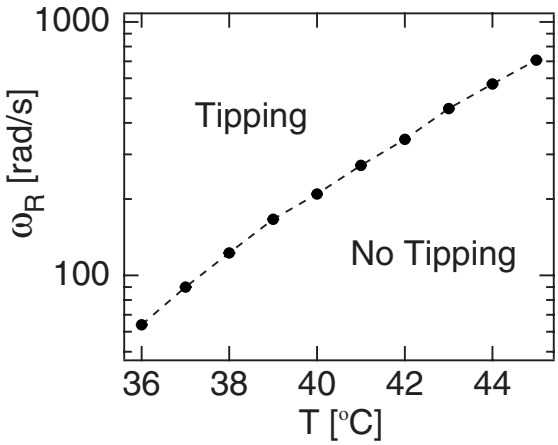

FIG. 3. Phase diagram specifying the rotation frequencies at which a nanowire of length 6 μm experiences a torque that causes it to tip out of the rotation plane as a function of temperature. The symbols indicate the minimum frequency at each temperature at which the wire tips out of plane following removal of the rotating magnetic field. The dashed line is a guide to the eye.

structed by identifying the minimum rotation frequency, shown by the solid circles, at which a wire of length 6.0 μm tips out of plane following the removal of the rotating magnetic field as a function of temperature.

For the results in Fig. 1, the external magnetic field used to rotate the wire overwhelmed this out-of-plane torque so that the measurements were essentially unaffected by $\Gamma_\perp$. However, when a smaller rotating magnetic field was employed, the magnitude of $\Gamma_\perp$ was comparable to the magnetic torque, and the wire tilted while rotating so that its long axis made a constant angle ϕ with respect to the plane in which the field rotated. We interpret the tilt angle ϕ as corresponding to the wire orientation at which $\Gamma_\perp$ was balanced by the magnetic torque that sought to rotate the wire back into the plane of the field, $\mu B \sin\phi$. Figure 2(c) shows $\Gamma_\perp$ as a function of ω_R for a wire with length $L=13.7$ μm at 30 °C. In the measurements B was tuned at each ω_R so that the wire maintained a fixed tilt angle $\phi=45°$. The resulting out-of-plane torque appears to follow an approximate power-law dependence on ω_R for $\omega_R > \omega_c$. ($\Gamma_\perp=0$ for $\omega_R < \omega_c$.) The solid line in Fig. 2(c) is the result of a power-law fit that gives $\Gamma_\perp \sim \omega_R^{0.40\pm0.05}$. Measurements on other wires and at other temperatures indicate that to within experimental uncertainty this power-law relationship is independent of wire length and temperature.

One possible source of $\Gamma_\perp$ is the normal stress difference N_1 created in the sheared solution. However, wormlike micelle solutions display a normal stress difference in both the linear and nonlinear shear regimes, and N_1 varies continuously with $\dot{\gamma}$ through the onset of shear thinning [10]. In contrast, the discontinuous onset of $\Gamma_\perp$ at ω_c suggests behavior indicative of a first-order transition. Thus, we speculate that the torque is associated with a transition to nematic order among the micelles in the shear-induced state, as proposed in previous studies [11,16,18]. Within this interpretation, the nonlinear shear of the rotating wire induces a nematic alignment in the form of a vortex. The wire, having created this nematic order, is also an impurity that distorts the order. Hence, the out-of-plane torque could result from a thermodynamic driving force that seeks to place the wire in the region of suppressed nematic order at the vortex core to reduce the free energy cost of its presence. This association of the out-of-plane torque with a nematic transition thus provides a natural explanation for the sudden onset of $\Gamma_\perp$at ω_c; however, more detailed information about the nematic order and its dependence on shear rate would be required to connect this scenario quantitatively to the dependence of $\Gamma_\perp$ on ω_R shown in Fig. 2(c).

C. Drag anisotropy

Regardless of the microscopic origin of the out-of-plane torque, the motion of the wire in response to it enables further investigations of the shear-induced state of the wormlike micelle solution. Specifically, time-resolved experiments tracking the wire as it tilts away from the rotation plane provide a measure of the drag that the fluid imposes in a direction perpendicular to the nonlinear shear flow. As an illustration, Fig. 4 shows results from a measurement in

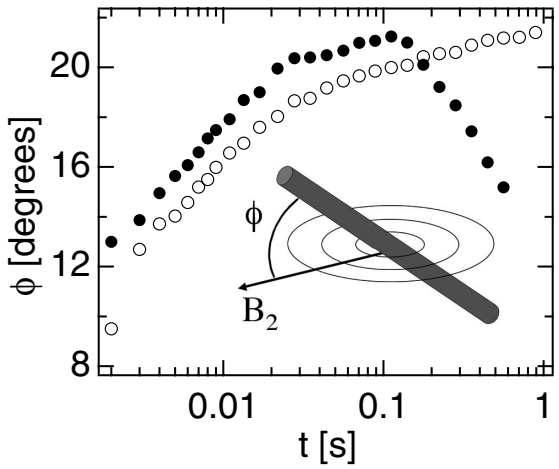

FIG. 4. Tilt angle ϕ of a wire of length 12.3 μm with respect to the plane of rotation after an 80 G rotating field is replaced with a stationary in-plane field $B_2=12$ G (solid circles). The inset shows a schematic of the tilted nanowire following the switch from the rotating field to B_2 with the concentric circles representing the plane of the rotation. ϕ increases at early times in response to the resultant torque from B_2 and the out-of-plane torque from the fluid. At late times ϕ decreases as the out-of-plane torque decays. Also shown is the angle of the wire as it rotates through quiescent fluid in response to a magnetic torque chosen to match this resultant torque (open circles).

which the tilt angle ϕ varies with time after the magnetic torque on a wire changes abruptly. The measurement was initiated by rotating a wire of length $L=12.3$ μm in the solution at 30 °C using a field $B=80$ G at $\omega_R=17$ rad/s, well above $\omega_c \approx 2$ rad/s. As the wire rotated to follow this field, it simultaneously tilted an angle $\phi \approx 7°$ from the field plane due to $\Gamma_\perp$. With this steady-state motion established, the rotating field was then suddenly removed at time $t=0$ and replaced with a small, stationary field $B_2=12$ G oriented in the plane of the rotating field. In response to this change, ϕ first increased due to the reduction in magnetic torque, as seen with the solid symbols at early t in Fig. 4. On a longer time scale, the out-of-plane torque decreased as the fluid returned to its quiescent state, and ϕ correspondingly decreased so that the wire aligned more closely with B_2, as seen at later t in Fig. 4.

To understand better the time dependence of this tilting, we show also in Fig. 4 results for the angle of the wire as it is rotated starting from rest in the quiescent fluid in response to a magnetic field. The magnitude and orientation of the field in this second measurement were chosen so that the torque matched the resultant torque from B_2 and $\Gamma_\perp$ in the measurement following rotation. Remarkably, the two curves have essentially identical shape over an extended range $0.003 < t < 0.1$ s. (The offset in ϕ between the data sets is consistent with the uncertainty in the asymptotic angle that would be reached in the absence of a decay in $\Gamma_\perp$.) This similarity in shape, which implies a similarity in angular velocity, indicates both that $\Gamma_\perp$ remains fairly constant after rotation ceases for $t < 0.1$ s and further that the drag on the wire is similar in the two measurements. At first glance one

might conclude from this similarity in the drag that the wire tilting in response to $\Gamma_\perp$ rotates through essentially quiescent material. However, since $\Gamma_\perp$ is intrinsically a feature of the nonlinear state of the fluid, the wire must still be under the influence of the shear-induced state. The similarity of the curves in Fig. 4 instead indicates a surprising feature of the nonlinear state, namely, an object moving in a direction perpendicular to the strong shear velocity (i.e., parallel to the shear-gradient direction) experiences a drag that is unchanged from the quiescent fluid despite the strong thinning that occurs for motion in the shear velocity direction. This observation thus illuminates in a direct way the anisotropic viscoelasticity of the nonlinear state of wormlike micelle solutions and further should set constraints on microscopic pictures of the nonlinear state.

IV. CONCLUSIONS

In conclusion, we have employed ferromagnetic nanowires to probe the nonlinear microrheology of a shear-thinning wormlike micelle solution. Among the key observations in this work are the qualitative differences between the drag on the wire and the macroscopic shear viscosity in the nonlinear regime. While such differences indicate the challenges posed for interpreting nonlinear microrheology results, they also suggest the potential of microrheology to access viscoelastic properties of complex fluids that are not readily apparent from conventional rheometry techniques. This new perspective is illustrated both by the temperature independence of the nonlinear drag in Fig. 1(a) and by the characterization of the out-of-plane torque on the nanowire in Fig. 2(c).

While extensions of microrheology into the nonlinear regime have been fairly limited to date, the development of these techniques in this direction is likely to become an area of increasing interest. For example, a topic investigated extensively with microrheology has been biopolymer networks such as *f*-actin, and a recent work using rheometry has indicated how the nonlinear behavior of actin best represents the mechanical response probed in measurements performed directly within biological cells [37]. As the work presented here shows, ferromagnetic nanowires can be especially effective probes of the nonlinear microrheology of complex fluids. The ability to apply strong and precisely controlled torques to the wires in suspension, and to change the magnitude and direction of these torques on rapid time scales, provides unique measurement capabilities, particularly with regard to flow-induced anisotropies, as illustrated in the "perpendicular" drag measurements in Fig. 4. Further experimental and theoretical work that helps establish the potential role for microrheology in characterizing the nonlinear viscoelastic properties of complex fluids would be most valuable.

ACKNOWLEDGMENTS

We thank R. Bandyopadhyay for assistance with the rheometry measurements and A. Belmonte and N. Handzy for helpful discussions. This work was supported by NASA through Grant No. NNC04GA69G and by the NSF through Grant No. DMR-0520491.

[1] R. G. Larson, *The Structure and Rheology of Complex Fluids* (Oxford University Press, New York, 1999).
[2] T. G. Mason and D. A. Weitz, Phys. Rev. Lett. **74**, 1250 (1995).
[3] B. Schnurr, F. Gittes, F. C. MacKintosh, and C. F. Schmidt, Macromolecules **30**, 7781 (1997).
[4] I. Y. Wong, M. L. Gardel, D. R. Reichman, E. R. Weeks, M. T. Valentine, A. R. Bausch, and D. A. Weitz, Phys. Rev. Lett. **92**, 178101 (2004).
[5] P. Habdas, D. Schaar, A. C. Levitt, and E. R. Weeks, Europhys. Lett. **67**, 477 (2004).
[6] T. M. Squires and J. F. Brady, Phys. Fluids **17**, 073101 (2005).
[7] A. Meyer, A. Marshall, B. G. Bush, and E. M. Furst, J. Rheol. **50**, 77 (2006).
[8] M. E. Cates and S. M. Fielding, Adv. Phys. **55**, 799 (2006).
[9] N. A. Spenley, M. E. Cates, and T. C. B. McLeish, Phys. Rev. Lett. **71**, 939 (1993).
[10] H. Rehage and H. Hoffmann, Mol. Phys. **74**, 933 (1991).
[11] J.-F. Berret, G. Porte, and J.-P. Decruppe, Phys. Rev. E **55**, 1668 (1997).
[12] C. H. Liu and D. J. Pine, Phys. Rev. Lett. **77**, 2121 (1996).
[13] R. Bandyopadhyay, G. Basappa, and A. K. Sood, Phys. Rev. Lett. **84**, 2022 (2000).
[14] R. Makhloufi, J.-P. Decruppe, A. Ait-Ali, and R. Cressely, Europhys. Lett. **32**, 253 (1995).
[15] R. W. Mair and P. T. Callaghan, Europhys. Lett. **36**, 719 (1996).
[16] J.-F. Berret, D. C. Roux, and G. Porte, J. Phys. II **4**, 1261 (1994).
[17] L. Becu, S. Manneville, and A. Colin, Phys. Rev. Lett. **93**, 018301 (2004).
[18] E. Fischer and P. T. Callaghan, Phys. Rev. E **64**, 011501 (2001).
[19] M. S. Turner and M. E. Cates, J. Phys.: Condens. Matter **4**, 3719 (1992).
[20] G. Porte, J. F. Berret, and J. L. Harden, J. Phys.: Condens. Matter **4**, 3719 (1992).
[21] P. D. Olmsted, Europhys. Lett. **48**, 339 (1999).
[22] N. Z. Handzy and A. Belmonte, Phys. Rev. Lett. **92**, 124501 (2004).
[23] N. Z. Handzy, Ph.D. thesis, Pennsylvania State University, 2005.
[24] M. Tanase, L. A. Bauer, A. Hultgren, D. M. Silevitch, L. Sun, D. H. Reich, P. C. Searson, and G. J. Meyer, Nano Lett. **1**, 155 (2001).
[25] C. Lapointe, A. Hultgren, D. M. Silevitch, E. J. Felton, D. H. Reich, and R. L. Leheny, Science **303**, 652 (2004).
[26] C. Lapointe, N. Cappallo, D. H. Reich, and R. L. Leheny, J. Appl. Phys. **97**, 10Q304 (2005).
[27] A. Anguelouch, R. L. Leheny, and D. H. Reich, Appl. Phys.

Lett. **89**, 111914 (2006).
[28] C. Wilhelm, J. Browaeys, A. Ponton, and J.-C. Bacri, Phys. Rev. E **67**, 011504 (2003).
[29] Z. Cheng and T. G. Mason, Phys. Rev. Lett. **90**, 018304 (2003).
[30] A. I. Bishop, T. A. Nieminen, N. R. Heckenberg, and H. Rubinsztein-Dunlop, Phys. Rev. Lett. **92**, 198104 (2004).
[31] A. Ortega and J. G. de la Torre, J. Chem. Phys. **119**, 9914 (2003).
[32] D. T. Chen, E. R. Weeks, J. C. Crocker, M. F. Islam, R. Verma, J. Gruber, A. J. Levine, T. C. Lubensky, and A. G. Yodh, Phys. Rev. Lett. **90**, 108301 (2003).
[33] While the rheometer performs stress-controlled measurements and the rotating nanowire corresponds effectively to strain-controlled conditions, studies of equimolar CPCl-NaSal using a strain-controlled rheometer report $\eta(\dot{\gamma})$ that is essentially the same as that in Fig. 1(b) [23].
[34] A. J. Levine and T. C. Lubensky, Phys. Rev. E **63**, 041510 (2001).
[35] H.-S. Dou and N. Phan-Thien, Rheol. Acta **42**, 383 (2003).
[36] L. M. Walker, P. Moldenaers, and J.-F. Berret, Langmuir **12**, 6309 (1996).
[37] M. L. Gardel, F. Nakamura, J. Hartwig, J. C. Crocker, T. P. Stossel, and D. A. Weitz, Phys. Rev. Lett. **96**, 088102 (2006).